COMPARISON OF ENERGY RESOLUTION OF DIFFERENT GAMMA RAY DETECTORS

A dissertation
submitted in partial fulfillment of the requirement for the award of degree of

Master of Science

in

Physics

Submitted by:

Arshjot Kaur

(301704003)

Under the supervision of

Dr. Sunil Devi

(Assistant Professor)

School of Physics and Material Science

Thapar Institute of Engineering and Technology (Deemed to be University)

Patiala-147004, (Punjab) INDIA

June-2019

Dedicated to my

Respected

Parents

And

Teachers

Certificate

This to certify that the report entitled 'COMPARISON OF ENERGY RESOLUTION OF DIFFERENT GAMMA RAY DETECTORS' submitted by Ms. Arshjot Kaur (Roll no. 301704003) of M.Sc. Physics, Thapar Institute of Engineering and Technology,(Deemed to be University), Patiala, was carried out by me under the supervision and guidance of Dr. Sunil Devi. I have not submitted this material for credit towards any other degree at Thapar Institute of Engineering and Technology, (Deemed to be University), Patiala or any other university.

Date: 17/06/2019

Arshjot Kaur
(Arshjot Kaur)

301704003

Sunil

Dr. Sunil Devi

Assistant Professor

SPMS, TIET

Patiala

Acknowledgment

I would like to express my sincere gratitude to all people who in some way or another motivated me through this dissertation. Foremost, I would like to thank my supervisor Dr. Sunil Devi for her motivation, devotion, patience and extensive knowledge. Her guidance has helped me in doing research and writing this dissertation.

I am truly thankful to my grandparents Mr. Kuldeep Singh and Mrs. Tej Kaur and my parents Mr. Narinderpal Singh and Mrs. Navdeep Kaur for their encouragement and support to follow my dreams. You are always there for me. I am especially grateful to my brother Gursimran, who always supported me emotionally and encouraged me to give my best.

I am thankful to my friends for listening and supporting me through this entire process. I would also like to thank Mr. Shoaib, Ph.D. Scholar, Thapar Institute of Engineering and Technology, who helped me with the basics of the analysis software and work related to the subject. I also want to acknowledge my gratitude towards all the faculty members of the School of Physics and Materials science who were always helpful. This accomplishment would not have been possible without them. Thank you.

Arshjot Kaur

Abstract

This master thesis aims to find suitability of gamma ray detectors for gamma rays in different energy regimes. For this purpose three gamma ray detectors: high purity germanium detector (HPGe), sodium iodide with thallium as an activator (NaI:Tl) and lanthanum bromide with cerium as an activator ($LaBr_3$:Ce_3) were studied. To identify the unknown radioisotopes or to know the excited states of the nucleus, we study their energy spectrum. For this purpose, there exist various kinds of the detectors according to the energy range of interest. The energy spectrum is calibrated with the known gamma rays to have the correct identification of the peaks. According to statistical theory, the shape of peaks is generally gaussian, so the spectrum is fitted with gaussian function to known Full Width at Half Maximum (FWHM) of every fitted peak. FWHM and energy of incident radiation are directly proportional to one another. The small value of FWHM corresponds to small peak width value showing less statistical fluctuations. Energy Resolution depends on FWHM. The detectors with better resolution can distinguish peaks more appropriately.

Table of Content

List of Figures

List of Tables

Chapter 1: Introduction

1.1 Introduction

There has always been a close connection between basic science research and technological advancements [1]. The concerns with nuclear accretion had resulted in the development of radiation detectors with superior energy resolution. With the introduction of thallium-activated sodium iodide scintillator, the route for gamma rays spectroscopy using small and portable detectors has been opened [2]. The early 1960s resulted in a revolution in gamma ray spectroscopy with introduction of semiconductor germanium (Ge) detectors that have the high-energy resolution.

The advantage of gamma ray detectors is that in addition to the detection of radioactivity and providing information about the nuclear structure, the information regarding excited states can also be attained. To induce the best conceivable energy resolution of gamma rays detectors, the electron-hole pair produced by ionizing radiation has to be studied as their statistics are greatly influenced by the properties of a material of the detector. The aim of this thesis to study the depiction of HPGe, NaI:Tl and $LaBr_3$:Ce_3. In this chapter, a brief introduction about the gamma rays and their interaction processes have been provided.

1.1.1: Radiation

The emission or propagation of the energy over space or material in the form of waves or particles is known as radiation. Radiation can be either ionizing or non-ionizing in nature. The ionizing radiation is more energetic and carry energy greater than 10 eV. The various types of radiations are given in Table 1.1.

Radiation Type	Example
Acoustic	Sound, Ultra sound, Seismic waves
Electromagnetic	Radio waves, Infrared, Ultraviolet, Visible light, Microwave, X-rays, Gamma rays
Particle	Alpha, Beta, Neutron radiations
Gravitational Radiation	radiation of the form of gravitational waves

Table 1.1: Types of radiations [1].

1.1.2: Electromagnetic Spectrum

EM spectrum is the chart covering electromagnetic radiation from 1 Hz to 10^{25} Hz frequency range, as shown in Fig.1.1.

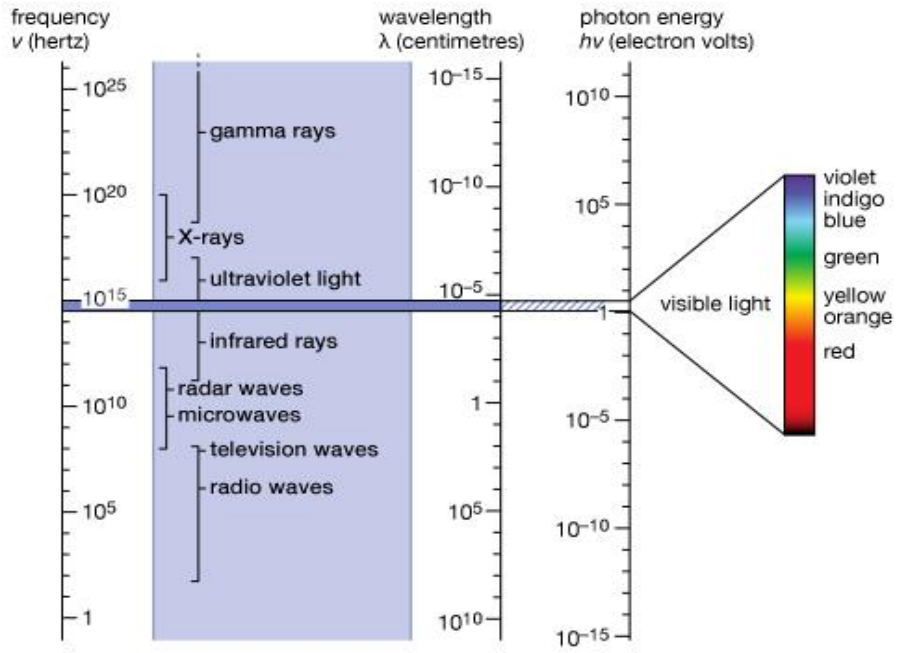

Fig. 1.1: EM Spectrum [7].

1.1.3: Gamma Rays

This thesis is about the detection of gamma radiation, which is a type of electromagnetic radiation and the most penetrating one. Its characteristics are given in Table 1.2.

Characteristics	Value
Energy	> 41.4 keV
Wavelength	$< 3 \times 10^{-11}$ meters
Frequency	$> 10^{19}$ Hz

Table 1.2: Characteristics of gamma rays [2].

- Discovery of Gamma Radiation

French Physicist and chemist Paul Ulrich Villard was the one to first observe gamma rays in 1900 when he was studying radiation from Radium, Polonium, and Uranium [3]. However, the name 'gamma' was given in 1914 by Ernest Rutherford. Also, he along with Edward Andrade showed that the gamma rays were electromagnetic radiation through the measurement of their wavelengths using crystal diffraction.

- Production of Gamma Radiation

For gamma ray emission nucleus must be in an excited (unstable) state and it may de-excite by emitting one or more photons of discrete energies to get stable, but the number of protons and

neutrons does not change [4]. Hence, remaining nucleus is of the same isotope but mainly of lower energy. Gamma ray emission generally occurs after alpha or beta decay.

- Gamma Radiation Interaction with the Matter

Detection of gamma radiation is based on the fact that how it interacts with the matter. The behavior of photons in the matter is dramatically different from that of charged particles. The major interactions of gamma rays in the matter are shown in Fig. 1.2, with their dependence on absorbers atomic number and energy range.

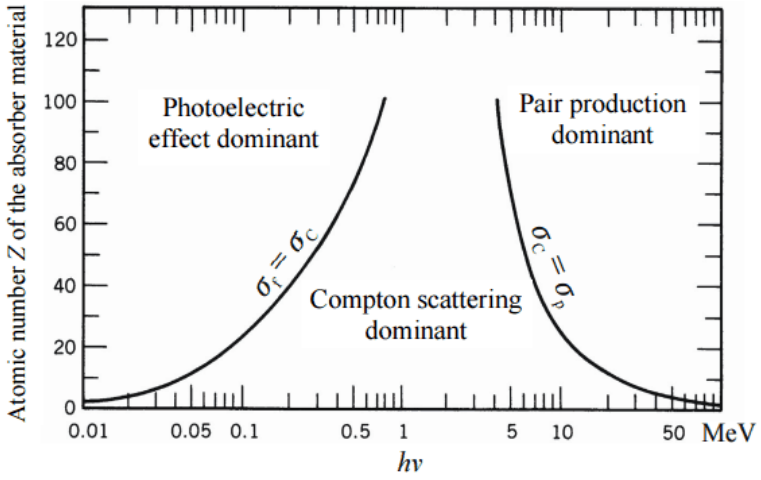

Fig. 1.2: Types of gamma ray interactions [8].

a. The Photoelectric Effect

The process where a photon delivers its entire energy to the constrained electron in an atom and then the electron of kinetic energy (E_e) equal to the difference between the incident photon energy (E_γ) and the binding energy (E_b) is emitted, this is known as photoelectric effect [5]. The process is described through Fig.1.3. The kinetic energy of the ejected electron is written as:

$$E_e = E_\gamma - E_b$$

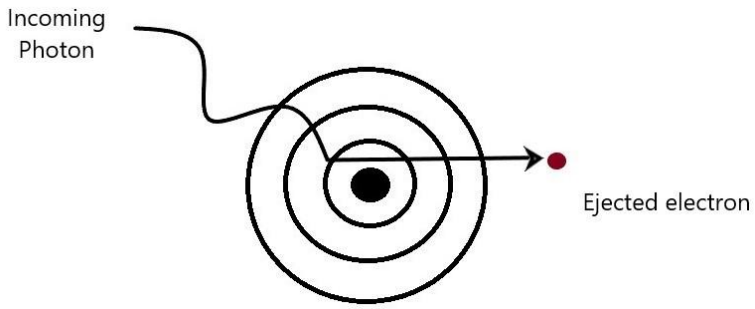

Fig.1.3: Photoelectric effect [9].

Full-energy peak (FEP) in the spectrum denotes the energy granted to emitted electron by incident photon. In the ideal case where there is only a photoelectric process a very sharp FEP is obtained. For momentum conservation, the photoelectric effect always occurs in the vicinity of the nucleus which absorbs the recoil momentum [5]. The probability of occurrence of photoelectric effect (P) is as $P \propto \frac{Z^3}{E^3}$, here Z denotes the absorber materials atomic number and E denotes incoming radiation energy.

b. The Compton Scattering

Compton scattering represents the case where there is only the scattering of gamma ray by an electron but not the absorption [5]. The process is described through Fig.1.4. If incident gamma ray energy is E_γ, the energy of the scattered gamma ray E_γ through an angle θ is given by:

$$E_{\gamma'} = \frac{E_\gamma}{1+\frac{E_\gamma}{mc^2}(1-COS\theta)}$$

Here,
m = scattered electron's mass
c = speed of light in vacuum
θ = angle of scattering

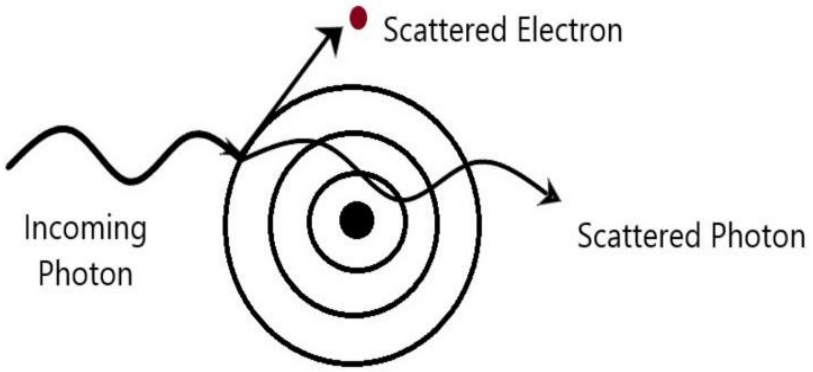

Fig.1.4: Compton scattering [9].

The energy of scattered electron describes the energy loss of the gamma ray which is minimum, (θ= angle of scattering) when $\theta = 0^0$ to a maximum when $\theta = 180^0$. In the spectrum pass on of maximum energy is shown by compton edge and while minimum energy via backscatter peak. The presence of a flat plateau is due to almost constant energy distribution of scattered electrons.

c. The Pair Production

It occurs only if the incoming gamma ray has minimum energy of 1.02 MeV, which is the rest mass of an electron-positron pair, and then the gamma ray is absorbed totally by producing an electron-positron pair. If the produced pair again interacts in matter, there is formation of pulse energy ($E-2mc^2$), where E denotes incoming photon energy and $2mc^2$ =1.02 MeV. Due to very brief life span of positron, it will immediately interact with an electron producing two photons of energy 511 keV each via its annihilation. The process is described through Fig.1.5. One of these

photons may be absorbed in the matter giving a peak of energy mc^2 =0.511MeV. The annihilation may occur even before the positron is completely stopped, the case when the peak energy will be higher [5].

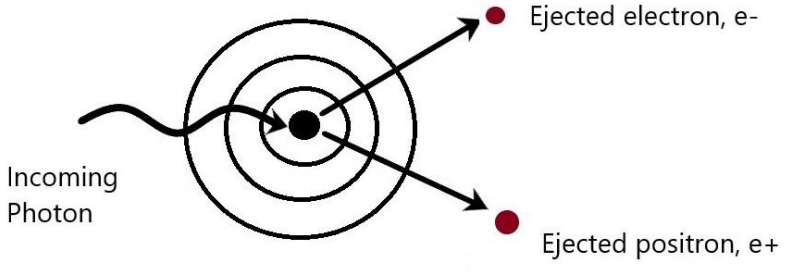

Fig.1.5: Pair production [9].

In the spectrum the peaks formed will be:

- A full energy peak (E) is formed in the spectrum if both of annihilation photons are absorbed.
- When only one is absorbed while the other is escaped, then one escape peak of energy E-mc^2 is formed.
- If both of them have escaped then we get double escape peak of energy E-$2mc^2$.

These interactions explain two principal qualitative features of gamma rays, which are:

i. Penetration power of the gamma radiation is much more than any other charged particle rays- which happens, as for the three major interaction processes the interaction cross section is very small than inelastic collisions of electron [6].

ii. There is only the attenuation in intensity of incoming photon beam while its passage through matter- It happens as the three major interaction results in removal of photon from beam via absorption or scattering. The photons, which do not suffer any interaction at all, pass straight through matter, hence they cling to their original energy. This all results in the cutback of total number of photons [6]. The attenuation suffered by the beam is as:

$$I(x) = I_0 \exp(-\mu x)$$

Where I_0 = intensity of incoming gamma ray beam
x= absorber material's thickness
μ=absorption coefficient

1.12: Literature Review

i. **Hossain, N. Sharip and K.K. Viswanathan, Scientific Research and Essays Vol. 7(1), 9 January 2012:** In this paper using gamma ray spectroscopy, efficiency and resolution of HPGe and NaI:Tl detectors were found. The dimensions of detector HPGe (GC2018) were a diameter

of 60.5 mm and length was 31.5 mm, while the dimensions of NaI:Tl detector (PRTEC 905-3) were 2"×2". The energy range of photo peaks used was 60 keV – 1300 keV. The efficiency and resolution were calculated using sources Cd-109, Co-60, Co-57, Te-123, Cs-137, Cr-51, Sn-113, Sr-137, Y-88. It was concluded that resolution was far better for HPGe, but in case of efficiency NaI:Tl was more effective.

ii. **D. Demir, M. Eroglu and A. Tursici, JINST 8 P10027, 2013:** This paper shows the study of characteristics of HPGe detector using elements Am-241, Ba-133, Cs-137 and Eu-152 in the energy range from 13.81 keV to 1212.95 keV. The full energy peaks were investigated by changing the distance between source and detector with an increase of 5 cm, from 5 cm apart to 20 cm apart. The dimensions of HPGe (planar configuration) were diameter = 16 mm, length = 10 mm, width of Be window = 0.12 mm, active area = 200 mm^2. The applied voltage was 1500 V. While calculating efficiency, there was a huge decrease at energies above 500 keV. It was concluded that HPGe has efficient resolution and with the reduction in background count a good efficiency can be achieved.

iii. **U. Datta Pramanik, Sunil Kalkal, Sujib Chatterjee, Characteristics of $LaBr_3$:Ce_3 scintillators and its comparison with other scintillators:** This paper shows the results of comparison of resolution of $LaBr_3$:Ce_3 detector with that of NaI:Tl scintillator. The experiment was performed at SINP, the sources used were Co-60 and Eu-152. It was found that the energy resolution of $LaBr_3$:Ce_3 was better at 3-4 % than that of NaI:Tl at 7-12 %.

iv. **Inaam Hani, Advances in Physics Theories and Applications, ISSN 224-719X(Paper), Vol.21,2013:** A investigation was done on two different sizes NaI:Tl detector using radioisotope Co-60. The sizes were 2”×2” and 1”×1.5”. It was concluded that as the size of detector increases, height and width of photopeak increases due to the increase in photon number. In addition, compton scattering probability increases with large detector volume.

v. **G.R. Pansare, S.J. Ansari and U.R. Kamthe, Research Journal of Material Sciences, Vol. 4(4), May 2016:** A NaI:Tl scintillator of size 2”×2” was studied to find detector resolution and efficiency. The source was kept at a distance of 3.7 cm from the detector and operating voltage was 750 V. The radioisotopes used were Ba-133, Co-60, Co-57, Na-22, and Cs-137. It was found that both the resolution and efficiency of the detector decreases with increase in gamma ray energy.

vi. **Elif Ebru Ermis, Gozde Tektas, Zuleyha Ozcelik, Cuneyt Celiktas, Jiri Pechousek**, **Radiation Science and Technology, Vol. 1, pp. 10-12, 2015:** A NaI(Tl) scintillator of dimensions 3”×3” was studied using Cs-137 source, to compare energy resolution from two different ways i.e. analog and digital. The detector was operated at 1000 V and the source was kept 4 cm apart from the detector. It was concluded that the resolution obtained from digitizer i.e. 6.80 % was better than from the analog method (MCA) i.e. 7.69 %.

vii. **P. Dorenbos, J. T. M. de Haas and C. W. E. van Eijk, IEEE Transactions on Nuclear Science, VOL.51, JUNE 2004:** A $LaBr_3$:Ce_3 detector formed using vertical Bridgman technique of the size 19"×19" was compared with same size NaI:Tl scintillator. Ba-133, Co-60, Co-57, Na-22 and Cs-137 were used for gamma ray spectroscopy. NaI:Tl has better resolution in the energy region less than of 100 keV, above this range $LaBr_3$:Ce_3 detector has far better energy resolution. There was found that decay time is very small (15-30 ns) in comparison to NaI:Tl. While photoelectric attenuation coefficient was similar for both scintillators, compton scattering and pair creation coefficient were larger for $LaBr_3$:Ce_3 by 40 % and 25 % respectively.

viii. **A. Kuhn, S. Surti, IEEE Nuclear Science Symposium Conference Record, 2005:** It talks about the TOF (Time of Flight) detector consisting of group of $LaBr_3$:Ce_3 detectors of size $4×4×30\ mm^3$, which is used in Positron Emission Tomography (PET) according to its property called Time of Flight (TOF) measurement. This property is due to its very rapid decay time (20-25 ns). A resolution of 5.1 % was measured at 511 keV. Monte Carlo simulations were used for simulation of spectra. It was concluded that with a time resolution of 200 ps, $LaBr_3$: (30 %) Ce_3 is a better choice for TOF detector in PET than $LaBr_3$: (5 %) Ce_3.

ix. **A. Giaz, L. Pellegri, S. Riboldi, F. Camera, N. Blasi, C. Boiano, A. Bracco, S. Brambilla, S. Ceruti, S. Coelli, F.C.L. Crespi, M. Csatlòs, S. Frega, J. Gulyàs, A. Krasznahorkay, S. Lodetti, B. Million, A. Owens, F. Quarati, L. Stuhl, O. Wieland, Nuclear Instruments and Methods in Physics Research,910-921, 2013:** In this paper $LaBr_3$:Ce_3 in cylindrical shape of size 3.5"× 8" was studied along with Hamamastu R10233-100SEL PMT. Mono-energetic gamma rays up to energy 2260 keV were used. There was the use of two kinds of voltage dividers i.e. E1196-26 a LABRVD, coupled to PMT. In the case of LABRVD, reduction in PMT dynode number or operating voltage was not required until 18 MeV. The energy resolution of 0.5-1 % was observed in high energy gamma rays.

1.3: References

[1]. M. Gelain, G. Maggioni, S. Carturan and D. De Salvador, D.R. Napoli, M. Loriggiola, D. Rosso and P. Cocconi, PoS (X LASNPA)042, 1-6 December 2013.

[2]. Glenn F. Knoll, Radiation Detection and Measurement, Third Edition, Chapter 10.

[3]. Leif Gerward, Phys. Perspect, 1999.

[4]. D.C. Tayal, Nuclear Physics, Chapter 7.

[5]. Glenn F. Knoll, Radiation Detection and Measurement, Third Edition, Chapter 2.

[6]. G. Nelson and D. ReWy, University of Washington:
http://faculty.washington.edu/agarcia3/phys575/Week2/Gamma%20ray%20interactions.pdf.

[7]. https://www.britannica.com/science/electromagnetic-spectrum.

[8]. R. D. Evans, The Atomic Nucleus, 1955.

[9]. R. Prasad, Nuclear Physics, Chapter 7.

Chapter 2: Theoretical Aspects

2.1: Detection of Gamma Rays

The first step to find out the response of any detector is the probability of interaction of gamma ray with the material of the detector, which is function of opted material's electron density. As gases have the lowest electron density, this rules out the possibility of using gas-filled detectors for gamma ray detection. Hence, the solid and liquid state detectors are used for gamma ray detection. This chapter discusses the two types of detectors on which work is done for this thesis i.e. HPGe and Scintillator Detector (NaI:Tl and $LaBr_3$:Ce_3).

2.2: High-Purity Germanium Detector, HPGe

2.2.1: Introduction

HPGe detector is the type of semiconductor detector. Until 1960s, silicon was used for gamma ray spectroscopy, but due to its small depletion width, merely of 1 mm, it was adequate only for soft X-rays and for few hundreds of keV energy range [1]. In the 1960s, the introduction of lithium drifted Germanium Ge(Li) led to the high-resolution nuclear spectroscopy, where the depletion width of few cm became available, making it suitable for detection of gamma rays of energy range of few MeV. In addition, as the atomic no. of Ge is larger than that of Si, attenuation coefficient in case of Ge is much larger making the mean free path much shorter. Hence, the preference of Ge over Si for gamma ray spectroscopy.
The depletion depth in a semiconductor is given as [2]:

$$d = \sqrt{\frac{2\varepsilon V_0}{eN}}$$

Where:

V_0 = reverse bias voltage
N = Intrinsic semiconductor's impurity concentration
ε = dielectric constant
e = electronic charge

For gamma ray spectroscopy, the large thickness value of detector is required, which means 'N' to be as small as possible, but if pure Si or Ge is used, the achievable 'd' will be of few mm, so 'N' needs to be as small as 10^{10} atoms/cm^3 to get 'd' of few cm. To reduce further impurity concentration, an impurity of the opposite type needs to be added for compensation. Both Ge & Si of p-type are of the purest form, thus the addition of donor atoms is required for compensation. Na, Li that are alkali metals are used for interstitial donors. This process is called ion drifting and we get Ge(Li) and Si(Li) detector materials. Lithium mobility in germanium at room temperature is very high which leads to the preservation of a Ge(Li) detector at liquid nitrogen temperature.

Another option to reduce impurity concentration is the formation of the high purity semiconductor crystal. In the 1970s, the first HPGe crystal was developed using zone refining technique, where low impurity level like 10^9 atoms/cm^3 was achieved.

2.2.2: Working Principle

HPGe detector is an intrinsic semiconductor detector, which works in a similar way as the solid-state ionization chamber. These detectors work in the fully depleted condition. When the radiation falls in depleted region, there is the production of electron-hole pairs. On the application of reverse bias in the active volume (depleted region), the electric field increases resulting in a larger drift of carriers making charge collection efficient.

2.2.3: Configurations

There are two types of configurations available for HPGe [1].

a) Planar Configuration

The planar configuration is also known as Π type configuration. In this configuration, with the use of lithium evaporation and diffusion, an n^+ electrical contact is made. There is the formation of the n+ p depletion region using reverse biasing. The opposite face is used as p^+ contact using acceptor ions implantation. HPGe detector is operated on the formation of full depletion width [1]. The representation of a planar configuration is shown in Fig. 2.1.

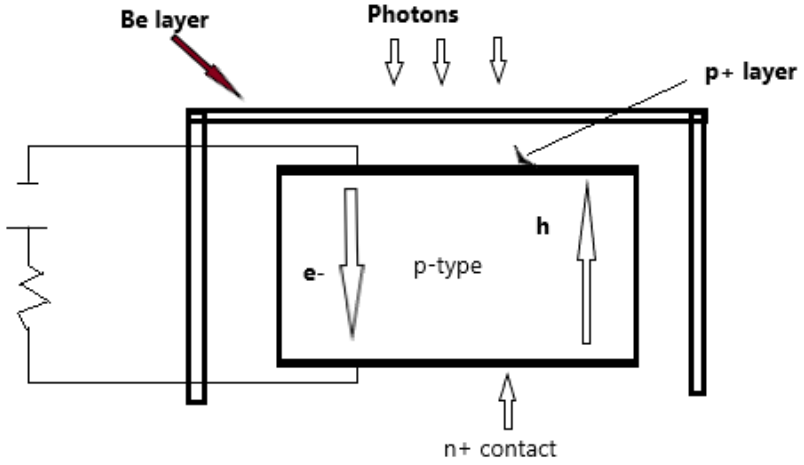

Fig 2.1: HPGe planar configuration [1].

b) Coaxial Configuration

In the case of planar configuration, the attainable maximum depletion depth is of the order of 1-2 cm; hence, the active volume of the detector is of the order 10-40 cm^3, which is not sufficient for

gamma ray spectroscopy [1]. To solve this problem a different approach was taken to construct the detector in the form of coaxial shape. In the coaxial configuration, on the outer side of cylindrical crystal made of germanium, an electrode is generated and the second one is made through the removal of the core. In this configuration, the attainable active volume is of the approximately 750 cm^3 [1]. The types of coaxial HPGe detectors are represented in Fig.2.2 and the cross-sectional view in Fig. 2.3.

Fig. 2.2: Coaxial configuration cross-sectional view [1].

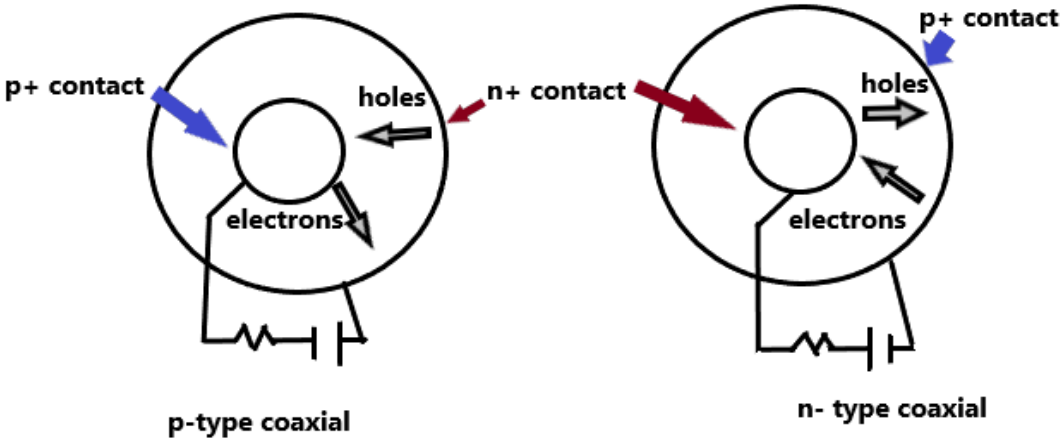

Fig. 2.3: Cross-section perpendicular to the cylindrical axis [1].

The semiconductor junction can be either inside or outside of the crystal according to germanium crystal type. It is generally preferred to keep the p-n junction on the outer side as for this configuration a lower depletion bias is needed.

2.2.4: HPGe detector operational characteristics (Cryostat and Dewar)

The band gap of germanium is 0.7 eV. Due to a very small band gap, at room temperature, there is the production of large leakage current, which is thermally induced. These conditions led to the working of the HPGe detector at liquid nitrogen temperature to reduce the noise [1].

The liquid nitrogen temperature (77 K) is accomplished via insulated dewar. Dewar is a basin of liquid nitrogen. The cryostat is a vacuum-tight container in which germanium crystal is kept [1]. This assembly is shown in Fig.2.4. The main function of the cryostat is to forbid the thermal conductivity between germanium crystal and air. The preamplifier is usually fitted to cryostat package for a reduction in capacitance. There are various configurations for cryostat and dewar [1].

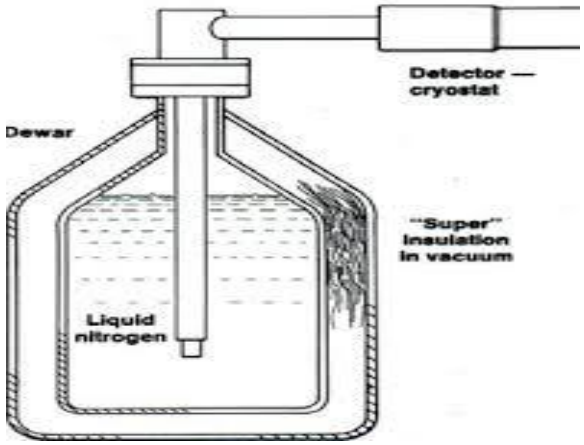

Fig.2.4: Cryostat-Dewar assembly [1].

2.3: Scintillation Detector

2.3.1: Introduction

The emission of light in the visible region by a certain kind of material refers to phenomenon called scintillation; the material is called scintillator, exhibiting the characteristic of luminescence [4].

The use of the scintillation process for detecting gamma rays is one of the oldest methods known to humankind. The very first record of this goes back to 1903 When Sir William Crookes observed light flashes on ZnS screen by alpha particles [4]. With the introduction of photomultiplier tube and an increase in the study of luminescence emitted from inorganic and organic particles, in 1945 this process again came to limelight [5, 6].

The material used as scintillator can be inorganic or organic crystals, organic liquids, and plastics. Organic material can be used in pure form and are chosen for beta spectroscopy while inorganic crystals are opted for gamma spectroscopy due to their large density value, but they cannot be used in the pure form [5]. The work in this dissertation is done using two types of inorganic crystals: NaI:Tl and $LaBr_3$:Ce_3.

2.3.2: Inorganic Scintillators

In inorganic materials, the crystal lattice determines the energy states. There is a forbidden band amid the fully filled valence band and empty conduction band. When radiation falls on material, electron acquires energy and jumps to conduction band causing the formation of a hole in the

valence band. The return back of electron by emitting photon to valence band will be inefficient in case of pure crystal and emitted photon will not lie in the visible region because of high energy. To overcome these problems an impurity called activator is added to increase the probability of photon emission in the visible range. This activator will create an energy state in a forbidden region via which an electron will de-excite. The energy band diagram after addition of thallium is shown in Fig. 2.5. The half-life of such energy states is of the order 50-500 ns [5]. Some examples of inorganic scintillators are NaI:Tl, ZnS:Ag, CsI:Eu, CsI:Tl, $LaBr_3$:Ce_3, etc. In the above examples element after ':' works as an activator.

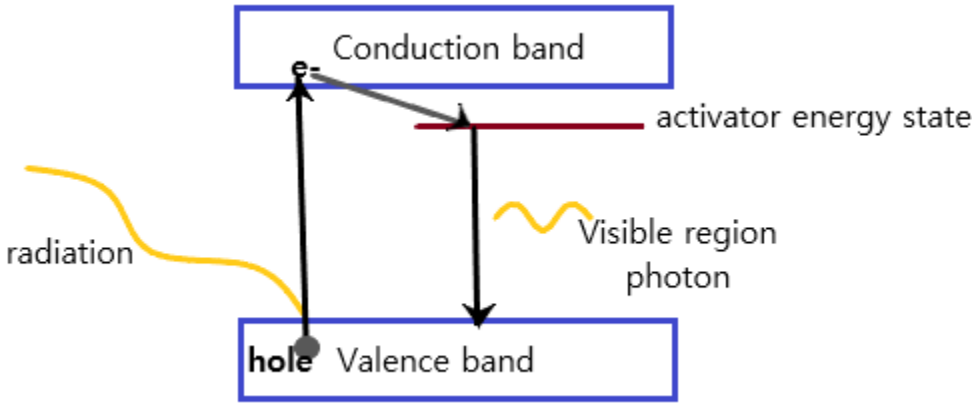

Fig.2.5: Energy bands of activated inorganic [5].

2.3.3: Sodium Iodide scintillator with Thallium activation, NaI:Tl

It is one of the most widely chosen inorganic scintillators for gamma ray spectroscopy. The very first use of NaI with thallium as activator was shown by Robert Hofstadter in 1948 [7]. The main property of NaI crystal is its light turnout is excellent, the light yield is 39000 photons/MeV. The crystal can be formed in a wide range of shapes and sizes, the largest formed crystal is of the diameter of 31 inches and its weight is 500 kg, which was formed at HORIBA factory in Arizona [4]. The properties of the NaI crystal are given in Table 2.1.

Properties	**Value**
Density (g/cm^3)	3.67
Relative light intensity	100
Refractive index	1.85

Table 2.1: Properties of NaI crystal [4].

The major drawback of this crystal is that it is hygroscopic and extremely fragile in nature. There is overlapping of emission and absorption spectrum in NaI crystal, to remove this thallium is added as impurity or activator to shift the emission spectra. Due to its hygroscopic nature, it is usually

kept in airtight carton mostly made up of aluminum. The arrangement of the crystal package is shown in Fig. 2.6.

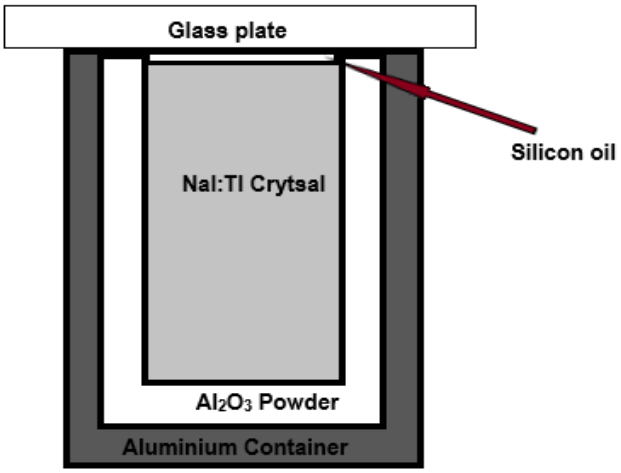

Fig. 2.6: NaI:Tl crystal mounted in aluminum container [8].

To limit the scattering of visible region photons, the crystal is first polished in a vacuum and then fixed in aluminum carton. For continuous passage of scintillation photon to PMT, the refractive index of glass is equated with a crystal using a very thin layer of DC-200 silicon oil is used [8]. To stop the leakage of an emitted photon in the surrounding, Al_2O_3 powder is used, as its refractive index is less than that of crystal, its reduce spillage of photons using total internal reflection.

2.3.4: Cerium activated Lanthanum Bromide scintillator, $LaBr_3$:Ce_3

Lanthanum bromide scintillator with cerium activator is a recent addition to the large group of the inorganic scintillator in the year 2001 [9]. The light turnout is large i.e. 61000 photons/MeV. Its density (5.1 gm./cm^3) is large in comparison to NaI:Tl (3.67 gm./cm^3). The time response is 15 ns i.e. decay constant is less than the NaI:Tl (230 ns) [10], which results in its use for fast timing applications and in finding the time of flight for positron annihilation tomography.

The lattice of $LaBr_3$:Ce_3 is of Uranium tri-Chloride (UCl_3) type and crystal structure of asymmetrical hexagonal type. Its thermal expansion coefficient is of non-isotropic nature, which results in the production of cracks in the cooling process of crystal formation [11]. Along with its advantages, it has a drawback of being hygroscopic, resulting in the need to keep the crystal in an aluminum airtight container as NaI:Tl crystal. Its cost of production is also high than other inorganic scintillators. Another shortcoming is the presence of intrinsic activity from La-138 isotope resulting in the production of 778 keV and 1435.8 keV gamma rays [10]. Alpha decays from Ac-227 in energy domain 4363 keV - 4960 keV contribute to background spectra [12].

2.3.5: Working of Scintillation Detector

The conventional representation of Scintillation detector is given in Fig. 2.7. The various parts of the detector are scintillator with the shielding of aluminum foil, photomultiplier tube, etc.

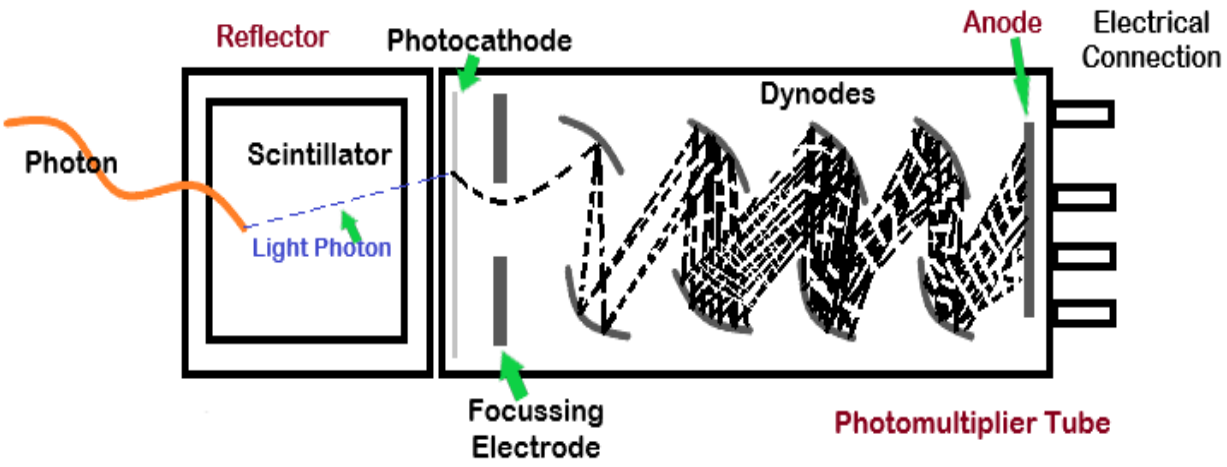

Fig. 2.7: Schematic diagram of scintillation detector [13].

Photomultiplier Tube (PMT):

PMT is an important component in working of the scintillation detector. Its outer covering is usually made up of glass to maintain the vacuum inside the tube. These are found in different shapes, which are shown in Fig.2.8.

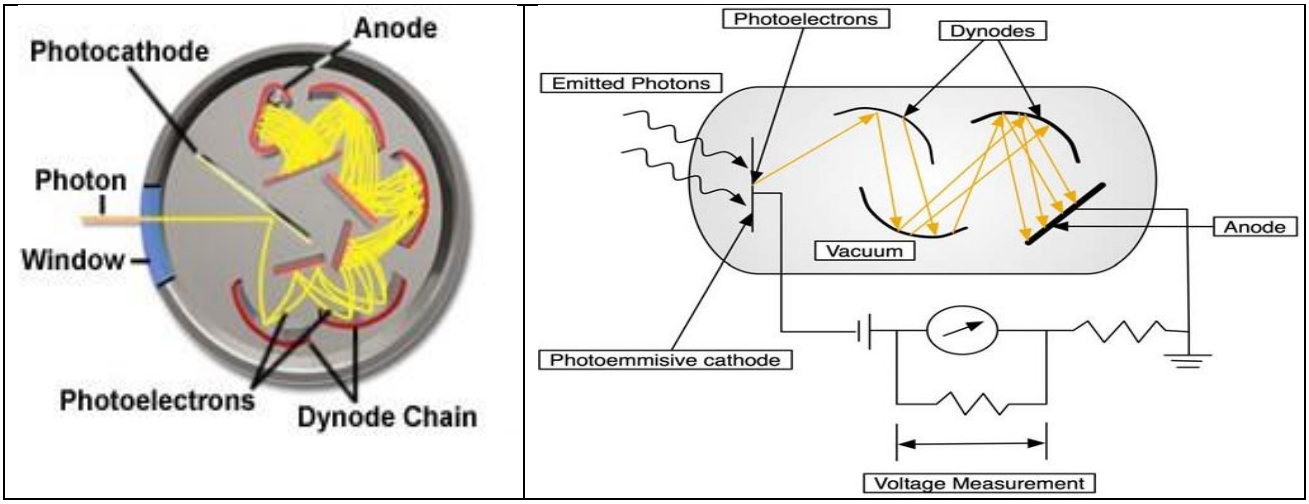

Fig. 2.8: Different designs of PMT [13].

The two processes i.e. photoemission and secondary emission decide the action of PMT. Photoemission is a process of converting visible region photons into electrons at photocathode, which is made up of alkali metals that have small work function for example cesium-activated antimony-rubidium. The photo emissive material absorbs the incoming photon and electron of photocathode absorbs this to breakout from the surface. The window of the photomultiplier tube is generally made of borosilicate glass.

The secondary emission occurs at dynodes, which are made from materials like Cs-Sb, Ag-Mg, etc. The kinetic energy of electron emitted from photocathode is very small in the order of 1-2 eV. So, the dynode material is chosen that has a band gap of the order of 1-2 eV, such that secondary emission of electrons may start. However, the number of electrons emitted is very small; to get the electron gain of high order ~ 10^7, this gain depends on applied voltage [13]. To get this desired result a number of dynodes with increasing positive potential are installed inside the photomultiplier tube. These electrons are then, collected at the anode and then current voltage transition is done through load resistance in the outer circuit.

2.4: Detector Response

In a detector, gamma ray photons can interact through any of the methods given in chapter 1. Multichannel analyzer (MCA) gives the spectral distribution in the form of pulse height spectra i.e. spectrum of the number of counts detected in a particular channel [3]. Then this spectrum is calibrated using sources of known energy example: Co-60, Cs-137, Na-22, etc. The selection of channel number depends on the resolution needed along with the number of counts detected. The spectrum obtained from MCA denotes the response function of any detector. Fig. 2.9 shows the Co-60 spectrum.

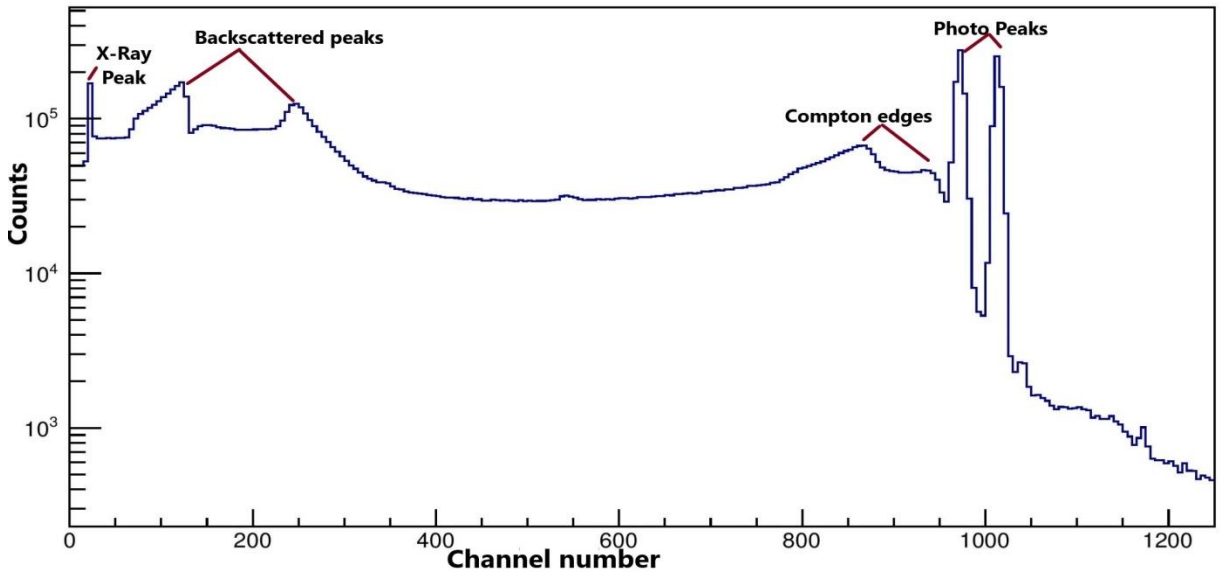

Fig. 2.9: Co-60 spectrum analyzed using root software**.**

a. Photopeak: It is also known as full-energy peak, which in the above spectrum corresponds to the energy value of 1173.2 keV and 1332.5 keV. This represents the events where gamma rays are fully absorbed and this is mainly due to the occurrence of photoelectric absorption. Another case is when there are few compton scattering before the occurrence of photoelectric absorption [3].

b. Compton Edge and Continuum: As the name suggests this is due to compton scattering, the peaks are shown in Fig.2.9 as compton edges represent the maximum energy disposed to scattered electrons. Energy detected depends on the scattering angle (θ) of the electron, which can be minimum for $\theta=0^0$ to a maximum at $\theta=180^0$, this results in the formation of a continuum in the spectrum [3].

c. Backscattered Peak: Some of the gamma rays that can interact via compton scattering with the material of the detector and are backscattered into detector before undergoing photoelectric absorption. The angle of backscattering is very large nearly equal to 180^o. The backscattered peak corresponds to the energy of the backscattered photon [3].

d. X-ray Peak: A characteristic X-ray can be seen in the spectrum if the surrounding material of the detector is ionized by gamma ray. This results in the knockout of inner shell electrons and outer shell electrons jump to the inner shell to fill the vacancy resulting in the formation of X-Ray [3].

e. Annihilation peak: This occurs only when the incoming gamma ray is of energy greater than 1.02 MeV, and then there is the possibility of occurrence of pair production near the nucleus, resulting in the formation of positron and electron pair, which annihilates immediately to form two gamma rays of equal energy i.e. of energy 0.511 MeV. If both of these interact with the detector, there is the formation of photo peaks, if only one interacts and other escape, we get single escape peak but if both escapes we get double escape peaks [3].

2.5: Energy Calibration

Calibration of energy is one of the most important steps while analyzing the gamma ray spectra. It provides us a relation between channel number (amplitude of output pulse from MCA) and energy deposited by gamma ray [1]. Many a time, the peaks of the spectrum obtained are already known, but when this is not the case, energy spectrum from a known source (Co-60, Cs-137, Am-241, etc.) is used to identify the peaks. Detector resolution is the one component, which decides to what accuracy peak centroid, can be localized [15].

2.6: Energy Resolution

In physics, resolution defines the resolving power. With gamma ray spectroscopy, resolution of any detector describes its power to resolve any two or more closely spaced peaks in the spectrum [15]. Poor resolution leads to large width peaks, showing a large amount of inconstancy while recording of data. Resolution is defined as the ratio of FWHM (full width at half maximum) and peak centroid (C). It is a dimensionless quantity.

There are various factors, which leads to fluctuations and hence inexact energy resolution. These factors may be due to noise generated from the instrumentation system, most dominant statistical noise from recorded signals diverse nature i.e. charge is generated through various carriers [14]. Generally, gaussian shape is assumed to be of pulse if, the only cause of fluctuation is statistical noise. Then with reference to Fig. 2.10, resolution (R) is defined as:

$$R = \frac{FWHM}{C}$$

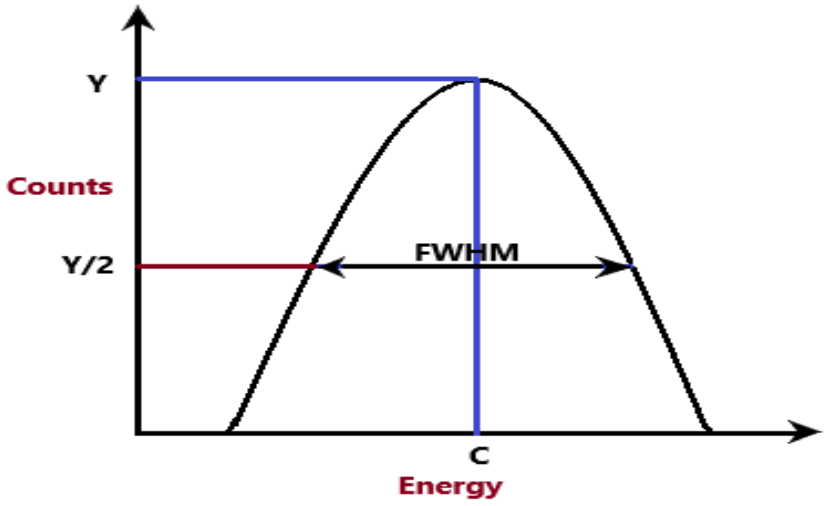

Fig.2.10: Gaussian curve [14].

2.7: References

[1]. Glenn F. Knoll, Radiation Detection and Measurement (Third Edition), Chapter 12.

[2]. D.V. Freck, J. Wakefield, Nature, 1960.

[3]. Glenn F. Knoll, Radiation Detection and Measurement (Third Edition), Chapter 10.

[4]. E.Joseph and R. Nasiru, Pelagia research laboratory, 2013.

[5]. Glenn F. Knoll, Radiation Detection and Measurement (Third Edition), Chapter 8.

[6]. D.C. Tayal, Nuclear Physics, Chapter 4.

[7]. G. Bellia, L. Cosentino, P. Finocchiaro, K. Loukachine, Nuclear Instrumentation Methods A 385,11997.

[8]. R. Prasad, Nuclear Physics, Chapter 7.

[9]. E. V. D. van Loef, P. Dorenbos, C.W. E. van Eijk, K. Krämer, and H. U. Güdel, Appl. Phys. Lett., vol. 79, pp. 1573–1575, 2001.

[10]. Pieter Dorenbos, Johan de Hass, C.W.E. Van Eijk, IEEE Transactions on Nuclear Science, June 2004.

[11]. F.G.A. Quarati , P. Dorenbos , J. van der Biezen, lan Owens, M. Sella, L. Parthier and P. Schotanus, Nuclear Instruments and Methods in Physics Research, A 729, 2013.

[12]. U. Datta Pramanik, Sunil Kalkal, Sujib Chatterjee, Characteristics of $LaBr_3$:Ce_3 scintillator and its comparison with other scintillator.

[13]. Glenn F. Knoll, Radiation Detection and Measurement (Third Edition), Chapter 9.

[14]. Glenn F. Knoll, Radiation Detection and Measurement (Third Edition), Chapter 4.

[15]. K. Szymanska, P Achenbach, M. Agnello, E. Botta, A. Bracco, Nuclear Instruments and Methods in Physics Research A 592, 2008.

Chapter 3: Experiment and Analysis Methods

3.1: NaI:Tl Detector

The NaI:Tl scintillation detector which was studied for this dissertation is newly purchased and located at P.G. Lab in School of Physics and Material Science, Thapar Institute of Engineering and Technology, Patiala, India. The detector was supplied by Nucleonix Systems PVT. LTD. Its specifications are listed in Table 3.1 [1]:

NaI:Tl scintillation detector	2"×2" well type
Lead Shielding	40 mm
Linear Amplifier	LA520
Multi-Channel Analyzer (MCA)	8K
Photomultiplier	EMI 9857

Table 3.1: NaI:Tl detector specifications.

Gamma reference set: The gamma ray sources used for this experiment were provided by BARC, India. The sources were placed at 5 cm distance from the detector. It contains gamma sources, evaporated and sealed in a plastic disk of dimension 25 mm (diameter) and 5 mm (width). The gamma sources used for this experiment are listed in table 3.2.

Gamma Isotope	Energy (MeV)	Formal Activity (μci)	Half-life (years)
Cs-137	0.662	2-5	30
Co-60	1.173,1.332	2-5	5.3
Na-22	0.511,1.280	2-5	2.6

Table 3.2: Gamma source set.

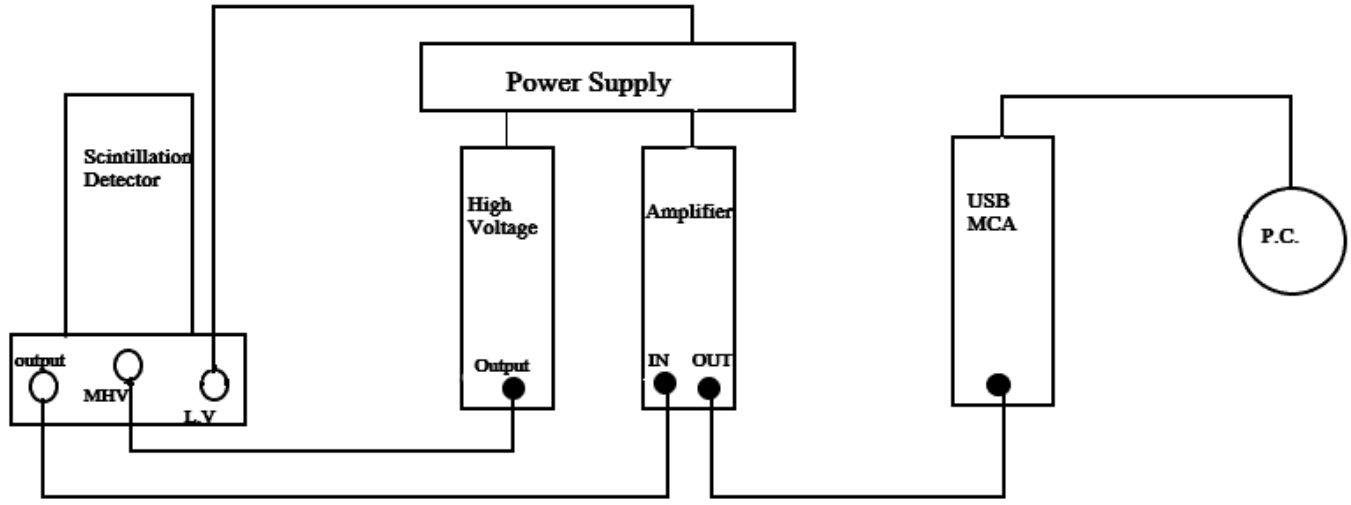

Fig. 3.1: Block diagram showing the NaI:Tl set-up [1].

Experimental setup: The setup for the experiment is shown in Fig. 3.2; the lead shielding is shown in Fig. 3.3 with multichannel analyzer in Fig. 3.4.

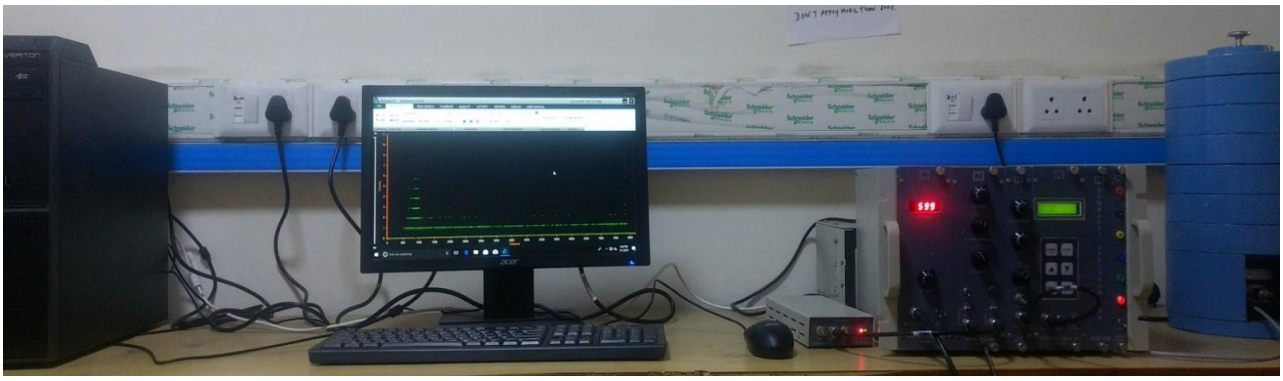

Fig.3.2: Experiment setup.

Fig.3.3: Lead shielding.

Fig.3.4: Multi-channel analyzer.

Energy calibration: Calibration of the acquired spectrum between channel number and counts is an important part of the analysis of gamma ray spectroscopy. To know the correct energy peak values,

the system needs to be calibrated using known energy sources. In this experiment, for energy calibration, Co-60 and Cs-137 were used. The system was made to run for 500 seconds (150 sec for Cs-137 + 350 sec for Co-60) with the high voltage unit (HV 502) operating at 600 V. The software used was ANUSPECT, which gives the spectrum of channel number vs. counts. The ANUSPECT used the following 2nd order polynomial for calibration:

$$E = a + bx + cx^2$$

where a, b, c are calibration coefficients and E corresponds to gamma ray Energy for particular channel number 'x'.

3.2: $LaBr_3$:Ce_3 Detector

The data of the experiment using $LaBr_3$:Ce_3 detector was provided by my supervisor Dr. Sunil Devi. The experiment was performed during her doctoral studies at the University of Delhi at the topic 'Investigation of Multinucleon Transfer Reactions and their effects on Fusion Reaction Mechanism around the Coulomb Barrier for Si-28+ Zr-90,94systems'. The dimensions of the detector were 9.84"×13.77". The source used for this experiment was Eu-152. For my dissertation, I used Software CANDLE and ROOT for energy calibration. The acquired spectrum from CANDLE was between channel number and counts and the gamma ray energy value for peaks of Eu-152 was found by using calibration formula: $E=a+bx+cx^2$, where a, b, c are calibration coefficients and E corresponds to gamma ray energy for particular channel number 'x'.

3.3: High Purity Germanium Detector, HPGe

The data of the experiment using HPGe detector was provided by my supervisor Dr. Sunil Devi. The experiment was performed during her doctoral studies at IUAC, New Delhi at the topic 'Investigation of Multinucleon Transfer Reactions and their effects on Fusion Reaction Mechanism around the Coulomb Barrier for Si-28+ Zr-90, 94 systems'. For my dissertation, I used software CANDLE and ROOT for energy calibration using source Eu-152. The channel number to Energy calibration was performed using formula: $E=a+bx+cx^2$, where a, b, c are calibration coefficients and E corresponds to gamma ray energy for particular channel number 'x'.

3.4: Reference

[1]. Nucleonix Systems PVT. LTD., Experimental Manual, MCA with ANUSPECT.

Chapter 4: Results and Discussion

4.1: High Purity Germanium Detector, HPGe Results

The resolution for HPGe detector was calculated for Eu-152 radioisotope. The calibration was performed with source Eu-152 in CANDLE (Collection & Analysis of Nuclear Data using Linux network) developed at IUAC (Inter-University Accelerator Centre), New Delhi, India. The decay scheme for Eu-152 is shown in Fig.4.1.

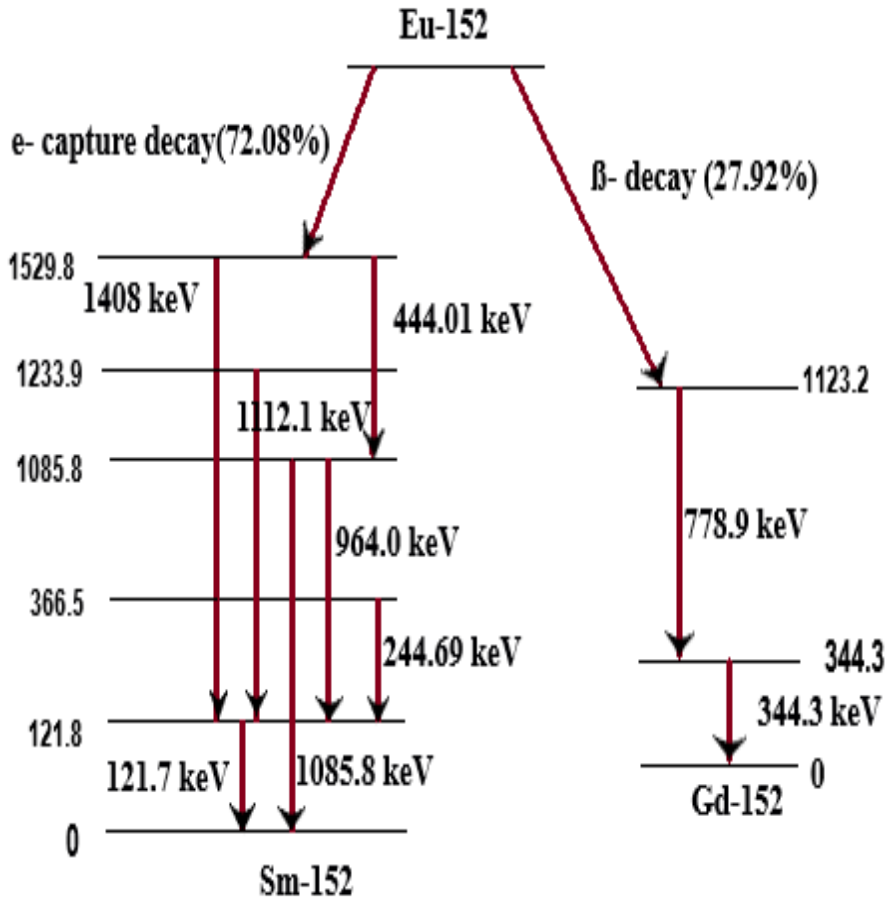

Fig.4.1: Decay scheme for Eu-152 [1].

Calibration parameters:

The gamma ray spectrum was gaussian fitted. The calibration parameters are listed in Table 4.1. Calibration equation for HPGe detector is: Energy = 4.1941e-07x^2+0.312349x-0.201497 (x=Channel number). Calibrated energy peaks are shown in table 4.1 and Fig.4.2. The gaussian fitted curve is shown in Fig.4.3.

Peak no.	Channel number	Energy (keV)
1	401.467	125.264
2	782.584	244.4947
3	1100.17	343.9424
4	1313.23	410.7072
5	1417.97	443.5437
6	2484.31	778.3575
7	2765.95	866.9498
8	3073.49	963.7627
9	3460.78	1085.7947
10	3544.36	112.1462
11	3865.06	1212.9966
12	4136.02	1298.8543
13	4478.57	1407.0878

Table 4.1: Calibrated energy peaks of Eu-152 from HPGe detector.

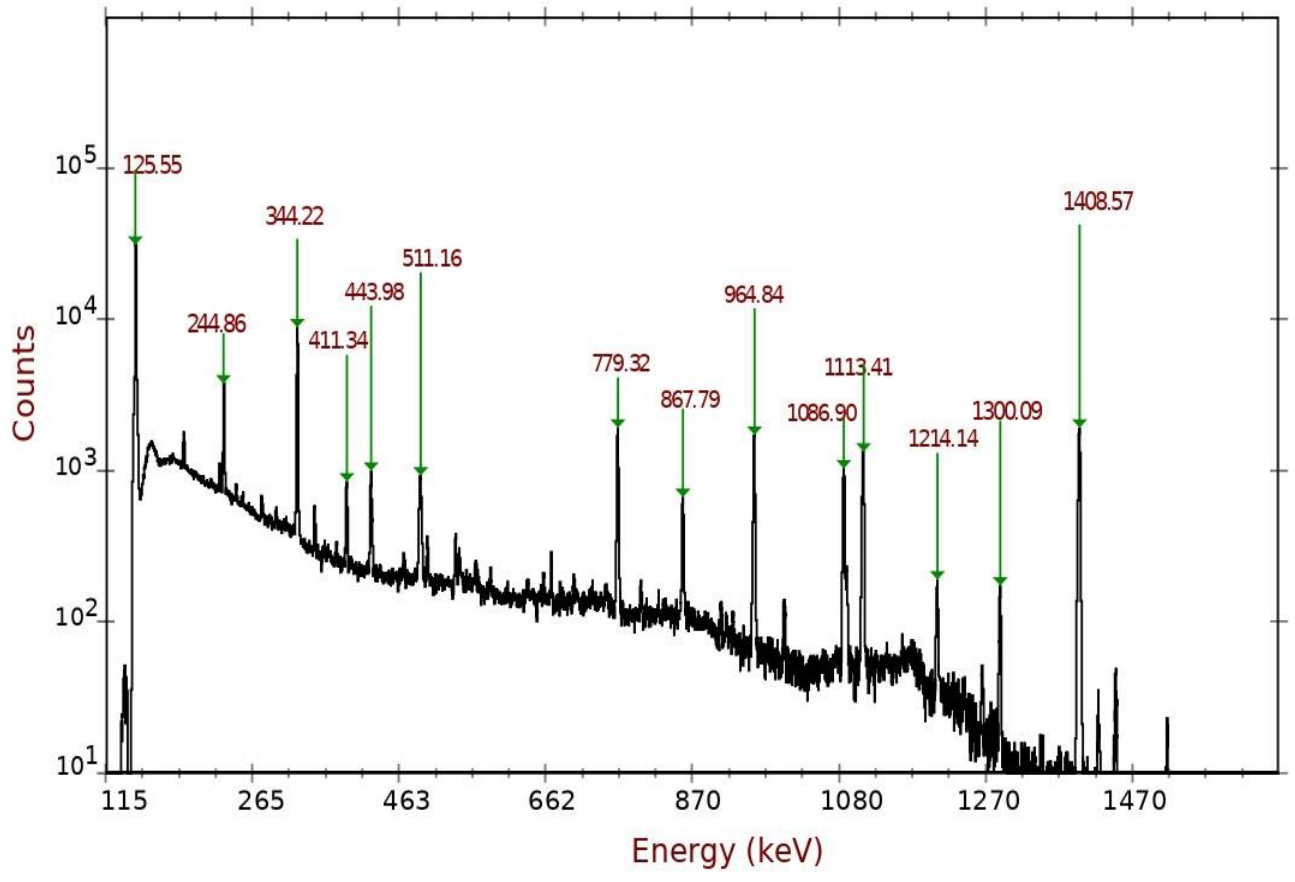

Fig.4.2 Calibrated energy spectrum of Eu-152 from HPGe detector with Calibration equation as: Energy = 4.1941e-07x^2+0.312349x-0.201497 (x=Channel number).

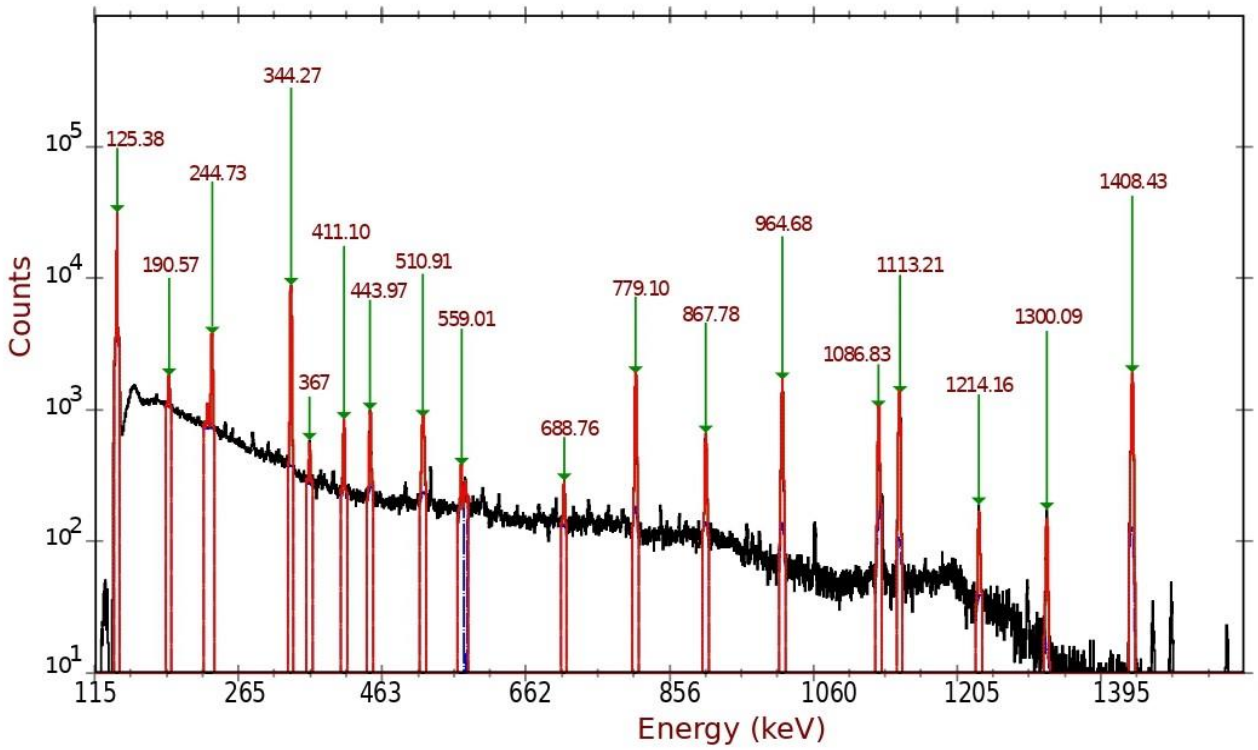

Fig.4.3: Gaussian fitted spectrum of Eu-152 for HPGe.

The calculated energy resolution for Eu-152 is given in Table 4.2 and Fig.4.4.

Peak	Peak Energy(keV)	FWHM(keV)	Resolution (%)
1	190.38	1.82	0.955982771
2	244.49	1.818	0.743588695
3	343.94	1.853	0.53875676
4	367.4	1.839	0.500544366
5	410.71	1.861	0.453117772
6	443.54	2.013	0.453848582
7	558.47	1.749	0.313177073
8	688.11	2.114	0.307218323
9	778.36	2.148	0.275964849
10	866.95	2.162	0.24938001
11	963.76	2.277	0.23626214
12	1085.79	2.248	0.207038193
13	1112.15	2.418	0.217416715
14	1213	2.386	0.196702391
15	1298.85	2.492	0.191862032
16	1407.09	2.66	0.189042634

Table 4.2: Energy Resolution of HPGe detector for different energies.

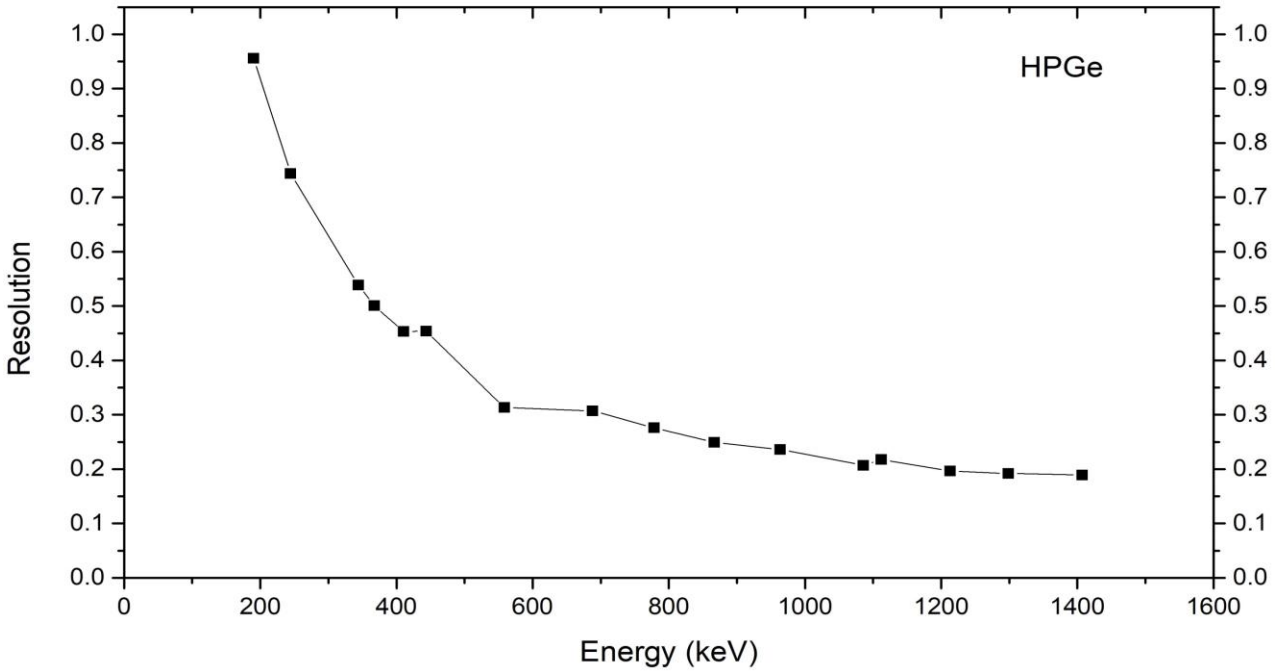

Fig.4.4: The plot of energy resolution for HPGe detector with radioactive source Eu-152.

4.2: NaI:Tl, Thallium activated Sodium Iodide Scintillation Detector results

To find the resolution for NaI:Tl detector,Cs-137, Co-60 and Na-22 were used. The Calibration was performed in ANUSPECT software using Cs-137 & Co-60 radioisotopes. The decay schemes for Cs-137, Co-60, and Na-22 are shown in Fig. 4.5, 4.6 and 4.7 respectively.

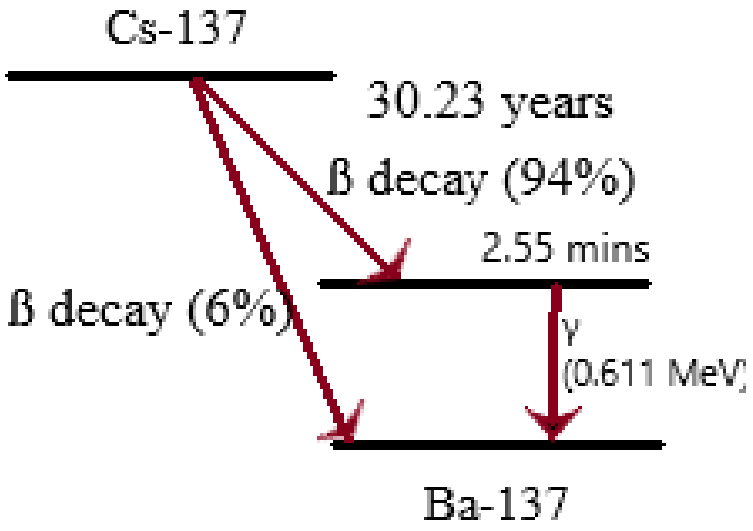

Fig. 4.5: Decay scheme for Cs-137 [1].

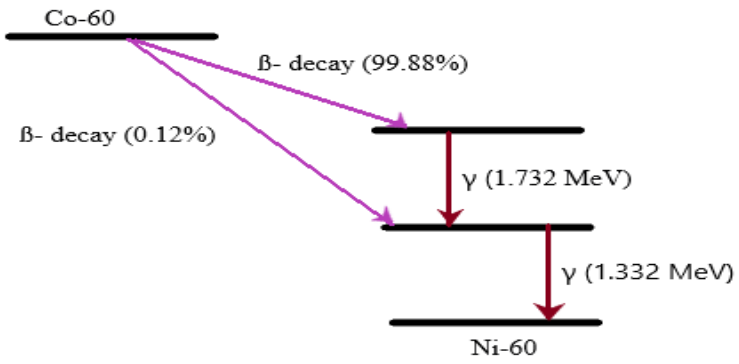

Fig. 4.6: Decay scheme for Co-60 [1].

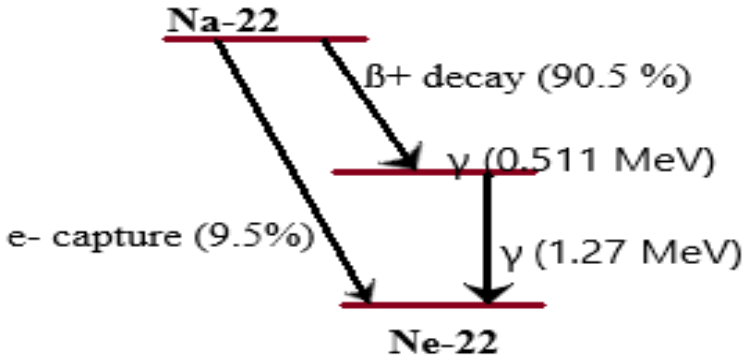

Fig. 4.7: Decay scheme for Na-22 [1].

The spectrum of Co-60 and Cs-137 is shown in Fig .4.8.

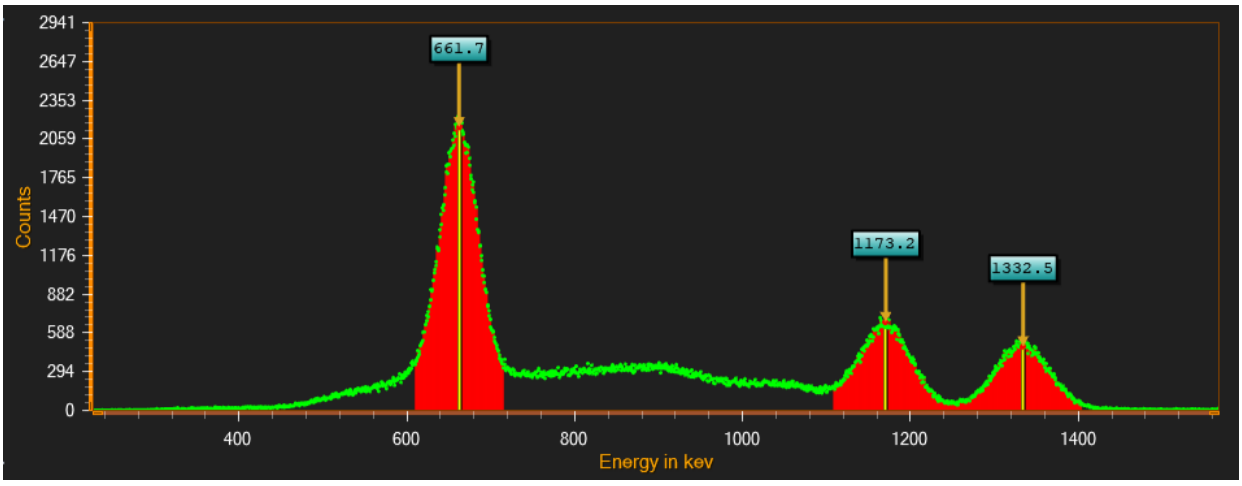

Fig.4.8 Cs-137 & Co-60 gamma ray spectrum from NaI:Tl detector.

The calibration equation obtained was: Energy = 0.8350465x – 100.7473, where 'x' denotes the channel number. The calibrated peak value along with calculated resolution are shown in Table 4.3.

Isotope	Peak Energy (channel)	Peak Energy (keV)	FWHM(channel)	FWHM(keV)	Resolution (%)
Na-22	740.1584	517.3195	42.8569	35.7875	6.917871837
Cs-137	913.4059	661.989	53.6733	44.8197	6.770459932
Co-60	1523.9127	1171.7906	76.1016	63.5483	5.423178851
Na-22	1648.1554	1275.5392	82.2513	68.6837	5.384679671
Co-60	1717.3864	1333.3501	85.0438	71.0155	5.326095524

Table 4.3: Energy resolution of NaI:Tl detector.

The graph showing the linear relation between channel number and energy is given in Fig. 4.9. The Na-22 gamma spectrum is shown in Fig. 4.10.

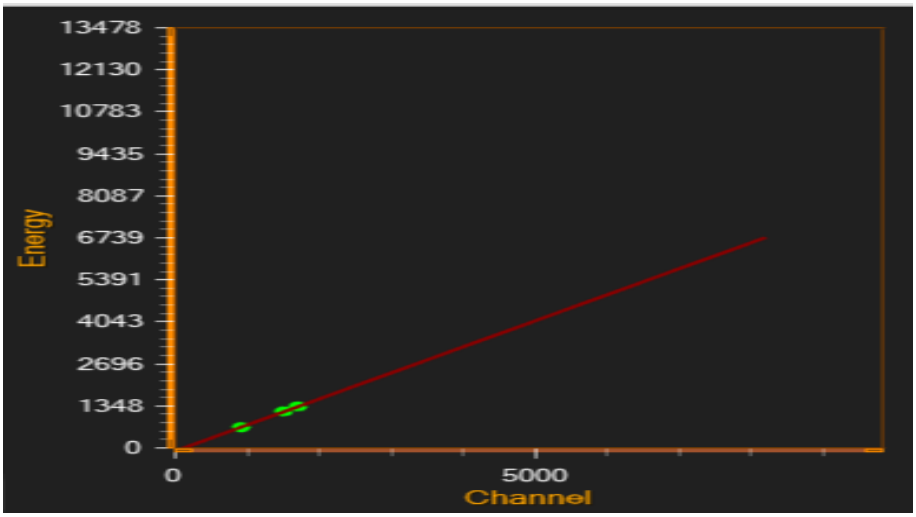

Fig. 4.9: Linear relation between channel number and energy after calibration.

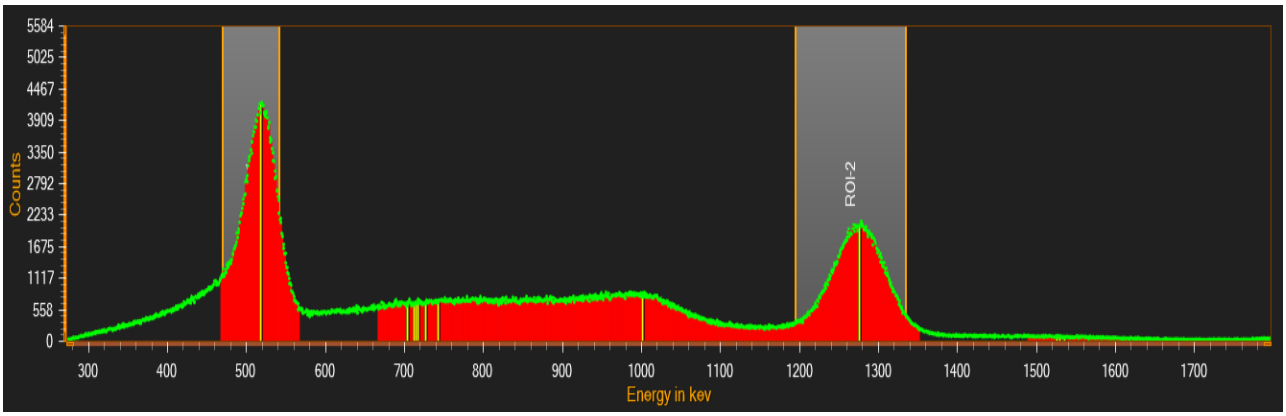

Fig. 4.10: Calibrated gamma ray spectrum of Na-22 showing regions of interest (ROI) of two gamma peaks.

The energy resolution curve for NaI:Tl scintillation detector is shown in Fig.4.11

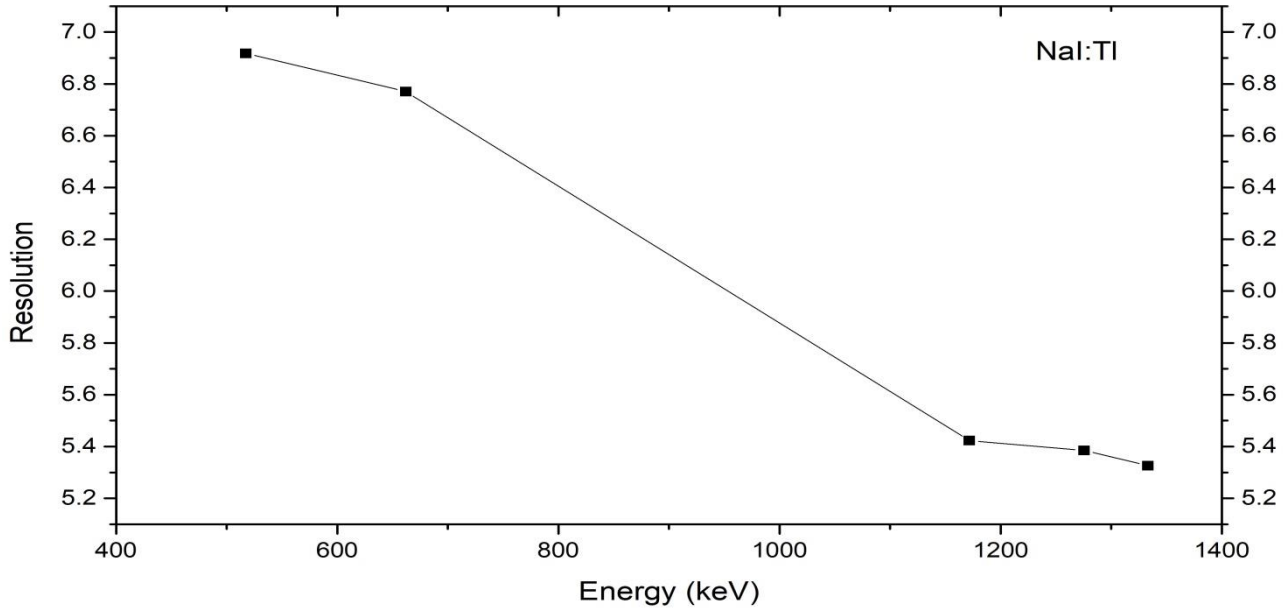

Fig.4.11: The plot of energy resolution as a function of gamma ray energy for NaI:Tl detector.

4.3: $LaBr_3$:Ce_3, Cerium activated Lanthanum Bromide Scintillation Detector results

The resolution for $LaBr_3$:Ce_3 scintillation detector was calculated using Eu-152 as a source and the gamma ray spectrum was analyzed in ROOT and CANDLE software. The spectrum was fitted with a gaussian curve and the calibration equation was $\underline{\text{Energy} = 0.000966796x^2 + 0.298279x + 80.2862}$, 'x' denotes channel number. The identified peaks are shown in Fig. 4.12 and table 4.4.

Peak no.	Peak Channel number	Peak Energy (keV)
1	140	140.99
2	270	232.12
3	377	330.15
4	443	404.47
5	478	444.98
6	761	868.94
7	822	979.83
8	876	1083.47
9	941	1217.05
10	1028	1408.16

Table 4.4: Energy peaks of Calibrated Gamma ray Spectrum of Eu-152 for $LaBr_3$:Ce_3 detector.

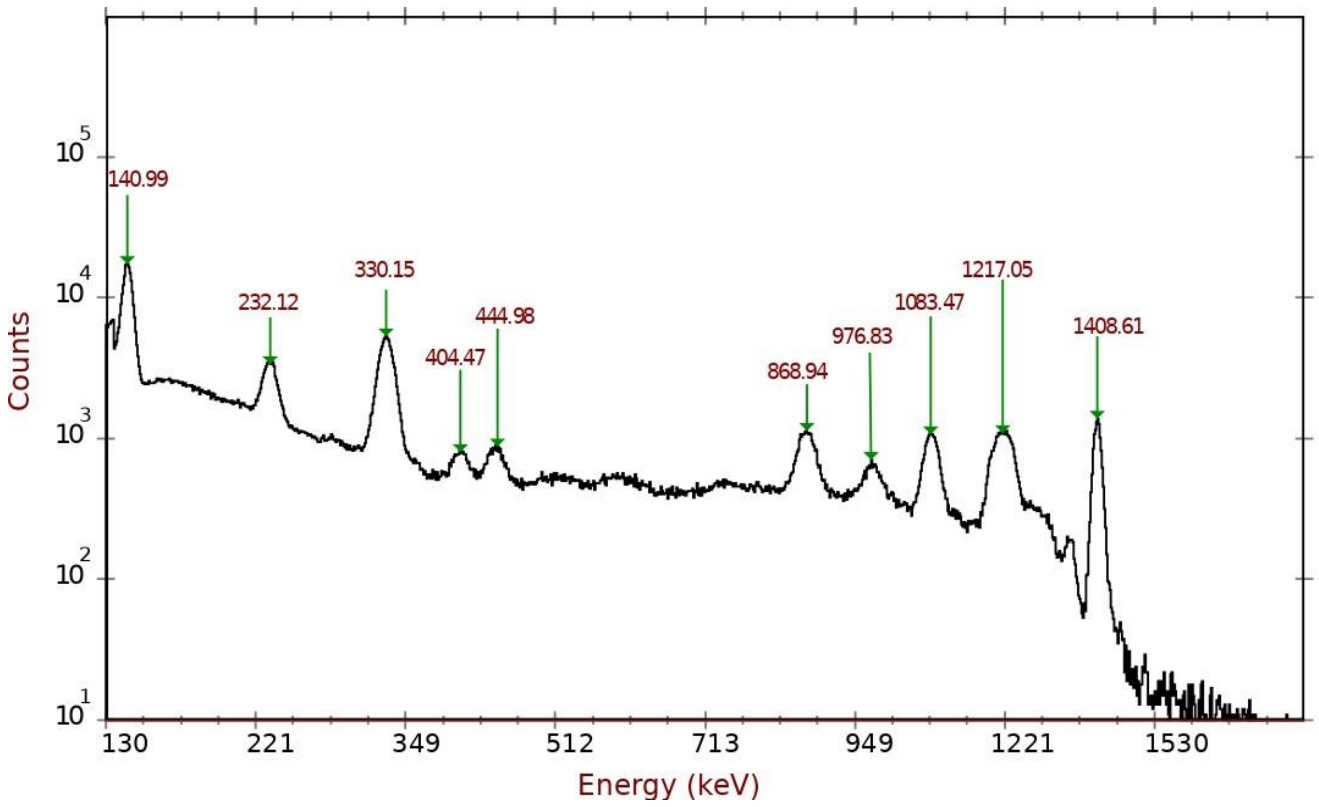

Fig. 4.12: Calibrated spectrum showing energy peaks of Eu-152 for $LaBr_3$:Ce_3 detector.

The gaussian fitted spectrum is given in Fig. 4.13. While the energy resolution calculation is given in table 4.5 and is plotted in Fig. 4.14.

Peak no.	Peak Energy (keV)	FWHM(keV)	Resolution (%)
1	107.6	5.199	4.831784387
2	140.99	2.888	2.048372225
3	232.12	4.396	1.89384801
4	265.08	6.262	2.36230571
5	330.15	4.864	1.47326970
6	404.47	5.636	1.39342843
7	868.94	5.498	0.63272492
8	976.83	4.936	0.50530798
9	1083.47	4.297	0.39659612
10	1217.05	6.842	0.56217903
11	1306.05	9.247	0.70801271
12	1335.74	9.247	0.69227544
13	1408.61	2.646	0.18784475

Table 4.5: Calculations for energy resolution of $LaBr_3$:Ce_3 detector.

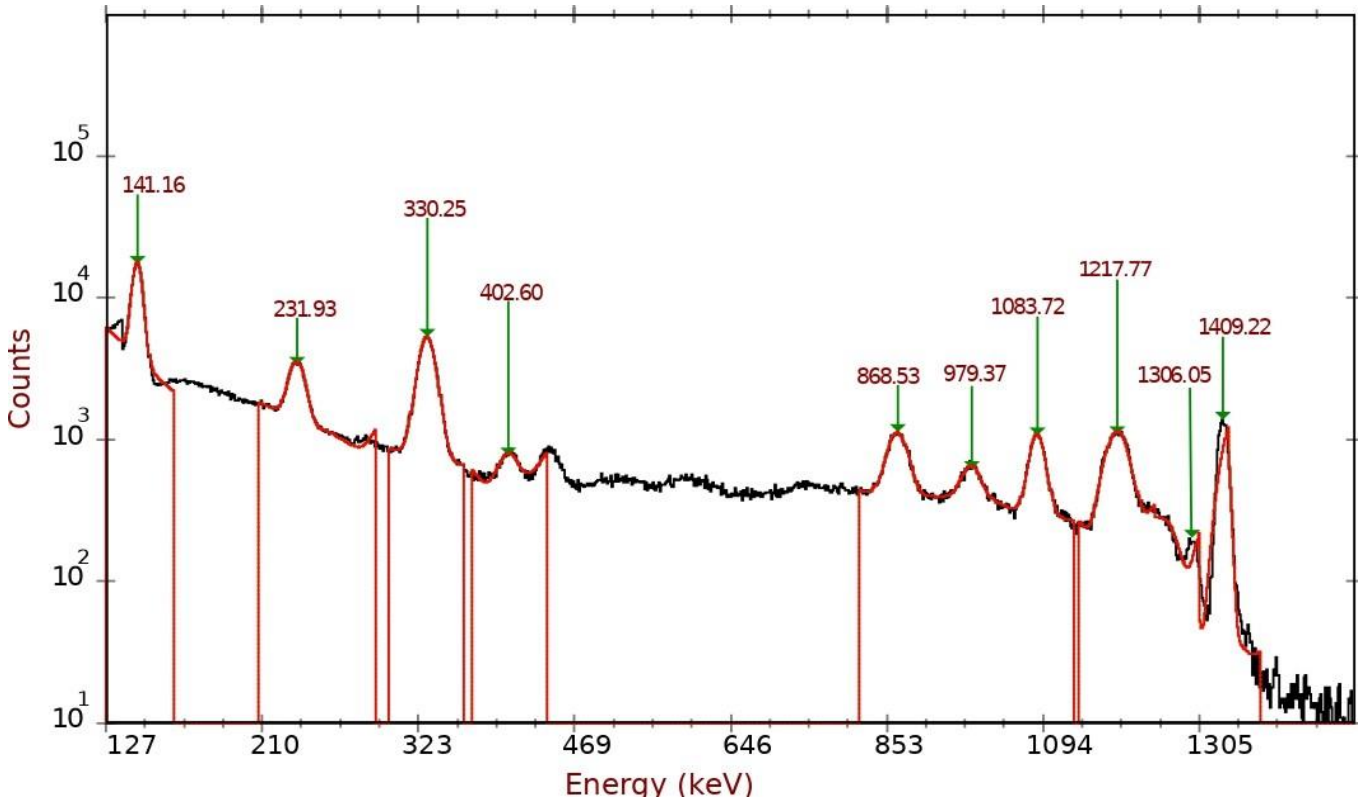

Fig. 4.13: Gaussian fitted gamma ray spectrum of Eu-152 of $LaBr_3:Ce_3$ detector.

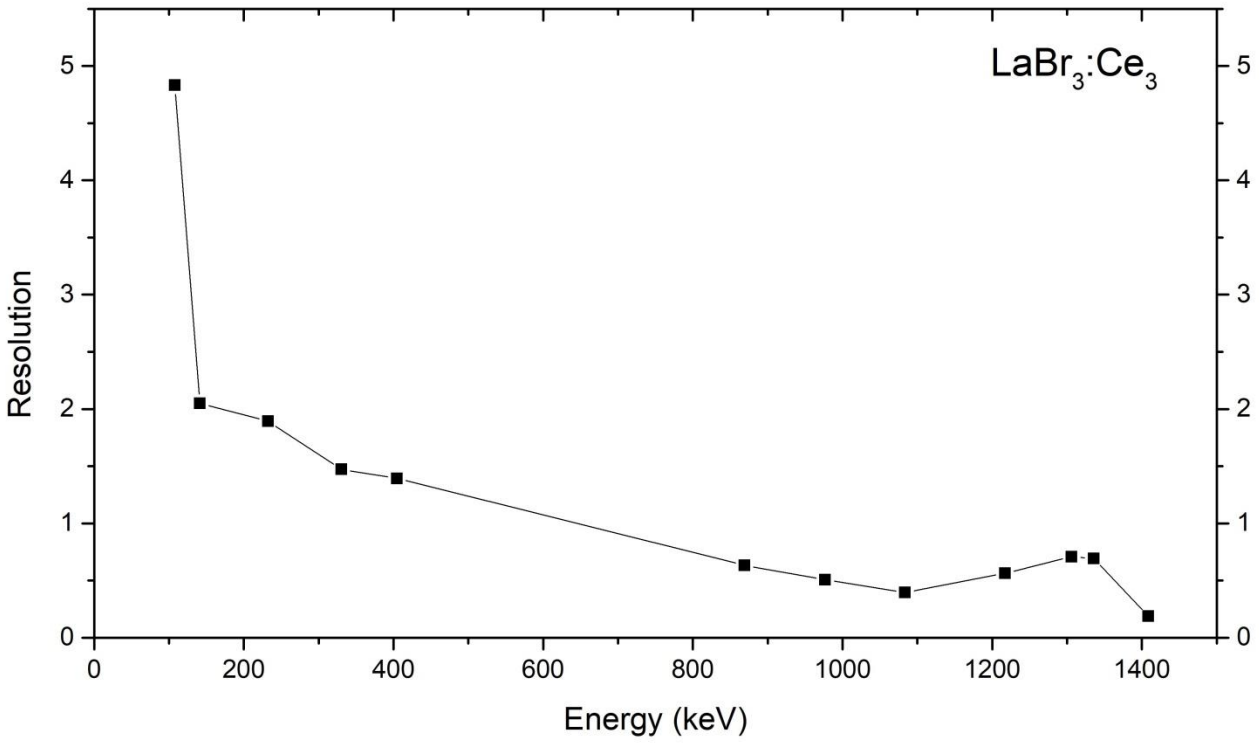

Fig. 4.14: The plot of energy resolution for $LaBr_3:Ce_3$ scintillation.

4.4: Discussion on Energy Resolution

To determine the relation between gamma ray energy and resolution of detectors, the energy spectrum was fitted with gaussian function and FWHM of fitted peaks were evaluated. A plot showing comparison of all the three detectors is given in Fig. 4.15. From the plot, it was concluded that with increasing gamma ray energy, the resolution becomes better for each detector.

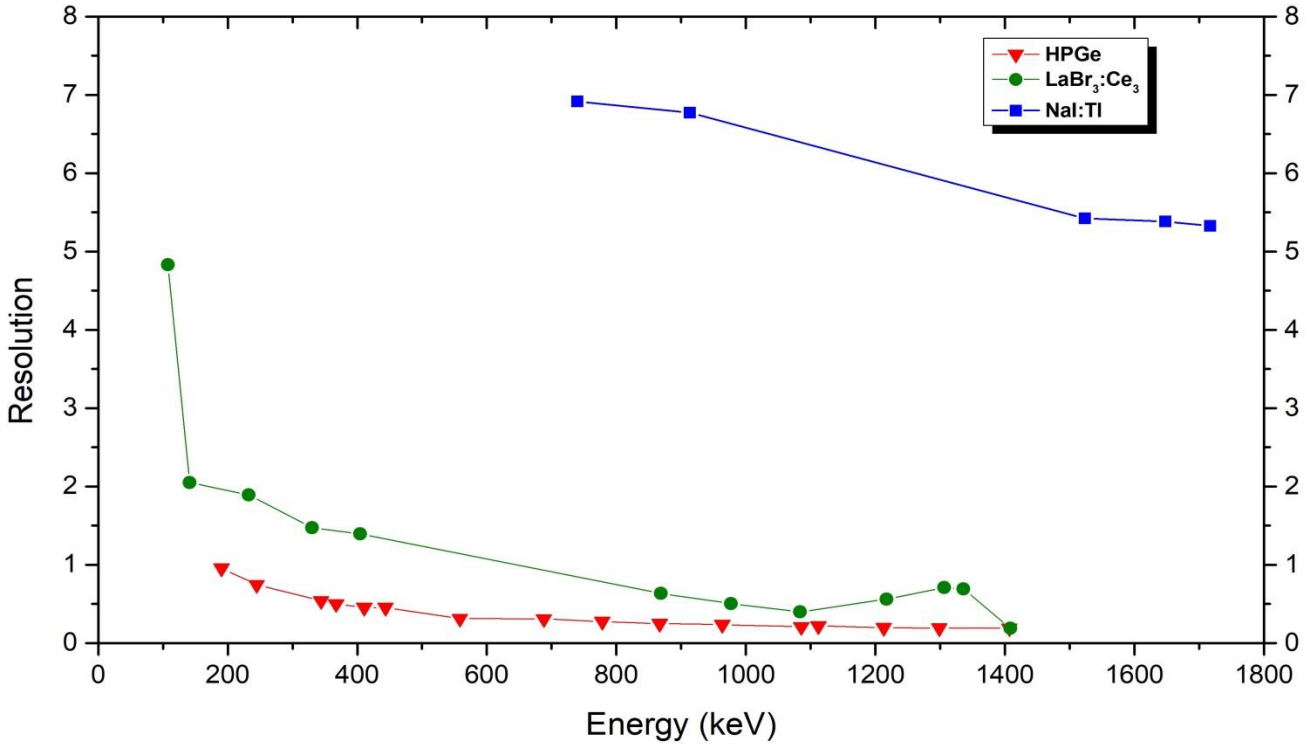

Fig. 4.15: A graph showing comparison of resolution for all the three detectors as a function of gamma ray energies.

The graph in Fig. 4.15 shows that HPGe has better resolution than NaI:Tl and $LaBr_3$:Ce_3. As already stated in the literature (review of literature is given in Chapter 1), HPGe is far better than the other two in terms of energy resolution. There are several factors like a statistical variation in the collection in charge carriers, noise from the electronic circuit, and drift in the response of detector, etc. that contributes to these results.

HPGe has band-gap of 0.7 eV and only requires 2.98 eV energy to produce a pair of electron-hole, while in the case of NaI:Tl the band-gap is 5.5 eV and need ~18 eV of energy to produce one pair of electron-hole, this number for $LaBr_3$:Ce_3 is band-gap of 3.75 eV and it requires at least three times the value of band gap energy to produce a pair of electron hole.

In semiconductor detector, photoelectric absorption is dominant interaction process, while in scintillation detectors one or more Compton scatterings occurs before photoelectric absorption, which results in nonlinear response function. The most dominant one is the statistical variation in the collection of information carriers. In the case of semiconductor detector, there is no need for the photocathode or photomultiplier tube, so the fluctuations related to the conversion of photons to electrons and multiplication of electron does not come into the picture. Therefore, there is a direct collection of electron-hole pair for pulse formation, which is not in the case of scintillation detectors.

The place of emission of visible region photon in scintillator also adds to nonlinearity in light yield, as it may again interact with atoms of material even before reaching the photocathode of PMT tube. The variation in the probability of generation of photoelectron by photocathode also contributes to the broadening of peak width.

4.4: References

[1]. https://www.nndc.bnl.gov/nudat2/.

Chapter 5: Conclusion

This chapter provides the major points of the project and the results obtained from the investigation. In this masters project, the work was to find the best available energy resolution of the gamma ray detectors i.e. high purity germanium detector (HPGe), sodium iodide with thallium as an activator(NaI:Tl) and lanthanum bromide with cerium as an activator ($LaBr_3:Ce_3$). The resolution of $LaBr_3:Ce_3$ is better than NaI:Tl, even if it belongs to the same group of inorganic scintillators which is due to its high light yield of 61000 photons/MeV while for NaI:Tl the number is 39000 photons/MeV. Its energy resolution is still worse than HPGe. In scintillations detectors, PMT is the main component, which results in expansion of the width of the peak due to inconstancy in the probability for detecting charge carriers. These fluctuations occur from the probability that whether a visible photon will be produced after de-excitation of electron of scintillator or whether this photon will reach photocathode and will result in emission of photoelectron. HPGe does not need any photomultiplier tube, so these fluctuations are not observed. Also, the energy required to produce electron-hole pair is small in semiconductor detector. Hence, large no. of charge carriers can be produced, resulting in better resolution in HPGe gamma ray detector. Still the resolution of HPGe is not perfect which may be due to presence of impurities acting as traps, resulting in imperfection in transportation of information carriers. Despite having better resolution, $LaBr_3:Ce_3$ is not cost effective and is more fragile than NaI:Tl crystal. However, if energy resolution along with simple circuitry is the concern, than $LaBr_3:Ce_3$ can be used to replace NaI:Tl and HPGe, due to the fact that it does not require the necessity of liquid nitrogen (dewar) especially at energies greater than 600 keV, resulting in non-complex circuitry and provides energy resolution more or less equal to that of HPGe gamma ray detector.

Turnitin Originality Report

arshjot-thesis by Arshjot Kaur

From MSc Thesis 2019 (MSc Thesis 2019)

- Processed on 12-Jun-2019 21:55 +0530
- ID: 1142962725
- Word Count: 7426

Similarity Index
8%
Similarity by Source

13/6/2019

Internet Sources:
4%
Publications:
5%
Student Papers:
5%

sources:

1 1% match (Internet from 29-Jul-2016)
https://air.unimi.it/handle/2434/229821?mode=full,6

2 < 1% match (publications)
Khater, Ashraf. "Radiation Detection Methods", Food Science and Technology, 2006.

3 < 1% match (Internet from 18-Sep-2018)
https://www.physics.rutgers.edu/grad/506/gamma.pdf

4 < 1% match (student papers from 16-Oct-2018)
Submitted to University of Witwatersrand on 2018-10-16

5 < 1% match (publications)
Review of Medical Dosimetry, 2015.

6 < 1% match (student papers from 04-Mar-2016)
Submitted to University of Wales Swansea on 2016-03-04

7 < 1% match (student papers from 19-Jan-2014)
Submitted to Middle East Technical University on 2014-01-19

8 < 1% match (publications)
Iliadis, "Nuclear Physics Experiments", Nuclear Physics of Stars, 02/02/2007

9 < 1% match (student papers from 13-Oct-2015)
Submitted to Higher Education Commission Pakistan on 2015-10-13